

# Effect of the double-counting functional on the electronic and magnetic properties of half-metallic magnets using the GGA+U method

Christos Tsirogiannis and Iosif Galanakis\*

Department of Materials Science, School of Natural Sciences, University of Patras, GR-26504 Patra, Greece

(Dated: April 12, 2018)

Methods based on the combination of the usual density functional theory (DFT) codes with the Hubbard models are widely used to investigate the properties of strongly correlated materials. Using first-principle calculations we study the electronic and magnetic properties of 20 half-metallic magnets performing self-consistent GGA+U calculations using both the atomic-limit (AL) and around-mean-field (AMF) functionals for the double counting term, used to subtract the correlation part from the DFT total energy, and compare these results to the usual generalized-gradient-approximation (GGA) calculations. Overall the use of AMF produces results similar to the GGA calculations. On the other hand the effect of AL is diversified depending on the studied material. In general the AL functional produces a stronger tendency towards magnetism leading in some cases to unphysical electronic and magnetic properties. Thus the choice of the adequate double-counting functional is crucial for the results obtained using the GGA+U method.

PACS numbers: 75.50.Cc, 71.20.Lp, 71.15.Mb

## I. INTRODUCTION

The rapid expansion of the field of spintronics and magneto-electronics brought magnetic materials at the nanoscale to the center of attention of modern electronics. The spin of the electron offers an additional degree of freedom in electronic devices with respect to conventional electronics based on semiconductors.<sup>1</sup> The design of magnetic nanomaterials with novel properties offers new functionalities to future devices, and to this respect *ab-initio* (also known as first-principles) studies of the electronic structure within density functional theory (DFT) play a crucial role allowing the modelling of the properties of several materials prior to their experimental growth. Among the most studied magnetic materials are the so-called half-metallic (HM) magnets,<sup>2,3</sup> which present metallic behavior for the majority-spin electronic band structure and semiconducting for the minority-spin electronic band structure. The ferromagnetic semi-Heusler compound NiMnSb was the first material for which the HM character was predicted and described,<sup>4</sup> and since then several HM compounds have been discovered.<sup>5-7</sup> The implementation of half-metallic magnets in devices is an active field of research (see Ref. 8 for a review of the literature).

DFT-based *ab-initio* electronic structure calculations using either the local-spin-density approximation (LSDA)<sup>9</sup> or the generalized-gradient-approximation (GGA)<sup>10</sup> for the exchange-correlation functional are quite successful for magnetic materials from weak to intermediate electronic correlations, but fail for systems with strong electronic correlations. There are two common ways to include correlations in first-principles electronic structure calculations. The first one is the so-called LDA+*U* scheme, in which the local-(spin)-density approximation (L(S)DA) of DFT is augmented by an on-site Coulomb repulsion term and an exchange term with the Hubbard *U* and Hund exchange *J* parameters, respectively.<sup>11,12</sup> Such a scheme has been applied for example to Co<sub>2</sub>FeSi, showing that correlations restore the HM character of the compound,<sup>13</sup> and to NiMnSb.<sup>14</sup> When the GGA functional is used instead of the L(S)DA the method is usually referred to as GGA+*U* scheme. A more elaborate modern computational scheme, which combines many-body model Hamiltonian methods with DFT, is the so-called LDA+DMFT method, where DMFT stands for Dynamical Mean-Field Theory.<sup>15,16</sup> LDA+DMFT has been applied to several HM magnetic systems like Co<sub>2</sub>MnSi,<sup>17</sup> NiMnSb,<sup>18-20</sup> FeMnSb,<sup>21</sup> Mn<sub>2</sub>VAI,<sup>22</sup> VAs<sup>23</sup> and CrAs.<sup>24,25</sup>

In the case of both LSDA+*U* (GGA+*U*) and LDA+DMFT schemes, the addition of the Hubbard *U* interaction introduces the need for a double-counting correction term in the energy functional to account for the fact that the Coulomb energy between the correlated states is already included in the LSDA (GGA) functional. Several double-counting schemes have been proposed in literature,<sup>26-28</sup> and in all proposed schemes an averaged energy for the occupation of a selected reference state is subtracted. Among the proposed functionals for the double-counting term, two are most commonly used: the so-called around-mean-field (AMF) functional and the atomic-limit (AL) functional; the latter is also referred to in literature as the fully localized limit (FLL) functional. The performance of these two functionals has attracted little attention in literature. In 2009 Ylvisaker and collaborators presented an extensive study on the effect of the two functionals when performing self-consistent LSDA+*U* calculations for several magnetic materials.<sup>29</sup> They have shown that the use of the LSDA+*U* interaction term usually enhances spin magnetic moments, but the AMF double-counting term gives magnetic states a significantly larger energy penalty than does the AL(FLL) functional and thus AL gives a stronger tendency to magnetism than AMF.<sup>29</sup>

## II. MOTIVATION AND COMPUTATIONAL METHOD

As mentioned above, ab-initio electronic structure calculations based on the mixed LSDA+U/GGA+U schemes as well as LDA+DMFT are widely used to study the influence of electronic correlations on the electronic and magnetic properties of half-metallic magnets. Thus the study of the influence of the double-counting term on the calculated properties for these materials is extremely important with respect to their potential use in realistic devices. The aim of the present study is to explore the effect of both AL and AMF functionals when performing GGA+U calculations with respect to usual electronic band structure calculations using the GGA functional for a wide range of half-metallic magnets (the reader is referred to Ref. 29 for an extended discussion on the exact formulation of the two functionals). To achieve our goal we have employed the full-potential nonorthogonal local-orbital minimum-basis band structure scheme (FPLO).<sup>30</sup> For the GGA calculations we have used the Perdew-Burke-Ernzerhof parametrization.<sup>10</sup> In the case of the GGA+U calculations the on-site Coulomb interactions for the correlated  $d$  or  $p$  orbitals are introduced via the  $F_0$ ,  $F_2$ ,  $F_4$  and  $F_6$  Slater parameters.<sup>31</sup> For all calculations a dense  $20 \times 20 \times 20$  grid in the reciprocal space has been used to carry out the integrals and both the charge density (up to  $10^{-6}$  in arbitrary units) and the total energy (up to  $10^{-8}$  Hartree) have been converged in each case.

In order to cover a wide range of half-metallic magnets in a coherent way, we have used in our calculations the ab-initio determined Coulomb effective interaction parameters (Hubbard  $U$  and Hund exchange  $J$  between localized  $d$  or  $p$  electrons) calculated in Ref. 32 using the constrained Random Phase Approximation (cRPA)<sup>33–36</sup> for 20 half-metallic magnets. We should note that (i) the determination of these parameters from experimental data is a difficult task, and (ii) the constrained local-density approximation (cLDA), although is the most popular theoretical approach,<sup>37–40</sup> it is well known to give unreasonably large Hubbard  $U$  values for the late transition metal atoms due to difficulties in compensating for the self-screening error of the localized electrons,<sup>34</sup> and thus cRPA which does not suffer from these difficulties, although numerically much more demanding than cLDA, offers an efficient way to calculate the effective Coulomb interaction parameters in solids.<sup>33,36</sup> We present results for all 20 half-metallic magnets studied in Ref. 32 which include representatives of the (i) semi-Heusler compounds like NiMnSb, (ii) ferrimagnetic full-Heusler compounds like Mn<sub>2</sub>VAL, (iii) inverse full-Heusler compounds like Cr<sub>2</sub>CoGa, (iv) usual L2<sub>1</sub>-type ferromagnetic full-Heusler compounds, (v) transition-metal pnictides like CrAs, and finally (vi)  $sp$ -electron (also called  $d^0$ ) ferromagnets like CaN. We have used the lattice parameters presented in Table 1 of Ref. 32. The Slater parameters entering the FPLO method are connected to

the Hubbard parameter  $U_{LDA+U}$  and to the Hund exchange  $J$  presented in Table II of Ref. 32 for the correlated  $p$ -states though the relations

$$F_0 = U_{LDA+U}, F_2 = 5 \times J, F_4 = F_6 = 0, \quad (1)$$

and for the correlated  $d$ -states

$$F_0 = U_{LDA+U}, \frac{F_2 + F_4}{14} = J, \frac{F_4}{F_2} = 0.625, F_6 = 0. \quad (2)$$

We should note here that  $U_{LDA+U}$  is an effective parameter depending both on the on-site intra-orbital Coulomb repulsion between electrons occupying the same orbital and on-site inter-orbital Coulomb repulsion between electrons occupying orbitals of the same  $\ell$  character but different  $m_\ell$  value. Thus, our study covers a wide range of half-metallic magnets allowing for a deeper understanding of the behavior of the AL and AMF double-counting functionals in the GGA+U calculated electronic and magnetic properties of different HM magnetic systems.

## III. RESULTS AND DISCUSSION

### A. Binary Compounds

We will start the presentation of our results from the binary compounds. There are two families of half-metallic binary compounds. The first includes the so-called  $sp$ -electron ferromagnets (also known as  $d^0$ -ferromagnets).<sup>41,42</sup> These compounds adopt the rocksalt cubic structure and have no transition-metal atoms in their chemical formula. We consider the nitrides and the carbides (CaN, SrN, SrC, and BaC) since they have the largest calculated Curie temperatures among the studied  $sp$ -electron ferromagnets.<sup>43–49</sup> Their total spin magnetic moment in units of  $\mu_B$  equals  $8 - Z_t$ , where  $Z_t$  is the total number of valence electrons in the unit cell; this behavior is known as Slater-Pauling (SP).<sup>50,51</sup> A detailed discussion on the origin of this rule and its connection to the half-metallicity can be found in Ref. 42. The usual GGA calculations produced for all four studied compounds a half-metallic state with total spin magnetic moments of  $1 \mu_B$  for the nitrides and  $2 \mu_B$  for the carbides. The results are gathered in Table I. The spin moment is carried mainly by the N and C atoms. Our calculated GGA results are similar to the GGA ones derived with the full-potential linearized augmented plane-wave (FLAPW) method as implemented in the FLEUR<sup>52</sup> code in Ref. 32. The use of the AMF within the GGA+U scheme leaves intact both the calculated spin magnetic moments and density of states (DOS) with respect to GGA calculations (we do not present the DOS since they are similar to the ones presented in literature). On the contrary the use of the AL functional has a tremendous effect on the calculated results. It produces an unreasonable and unphysical charge transfer from the Ca(Sr,Ba)

TABLE I: Atom-resolved and total spin magnetic moment per formula unit for the XY binary compounds. Results have been obtained within the FPLO method<sup>30</sup> using the GGA functional for the exchange interaction potential<sup>10</sup> and the GGA+U scheme employing both the atomic-limit (AL - also known as fully-localized-limit FLL) and the around-mean-field (AMF) functionals for the double counting term. Values for the on-site Coulomb and exchange parameters are the ab-initio determined ones within the constrained Random-Phase-Approximation (cRPA) in Ref. 32. Lattice constants are the ones presented in Table 1 in the later reference. Note that for the compounds which do not contain transition metal atoms (known as d<sup>0</sup>-ferromagnets) GGA+U within the AL functional gives unrealistic results.

Comp.	Functional	$m_X$	$m_Y$	$m_{\text{total}}$
CaN	GGA	-0.065	1.065	1.000
	GGA+U (AL)	11.836	-4.836	7.000
	GGA+U (AMF)	-0.065	1.065	1.000
SrN	GGA	-0.072	1.072	0.999
	GGA+U (AL)	16.363	-9.362	7.000
	GGA+U (AMF)	-0.072	1.072	0.999
SrC	GGA	-0.004	2.004	1.999
	GGA+U (AL)	15.578	-9.578	6.001
	GGA+U (AMF)	-0.004	2.004	1.999
BaC	GGA	0.057	1.943	2.000
	GGA+U (AL)	3.261	0.378	3.999
	GGA+U (AMF)	0.057	1.943	2.000
VAs	GGA	2.427	-0.427	2.000
	GGA+U (AL)	2.415	-0.415	2.000
	GGA+U (AMF)	2.151	-0.151	2.000
CrAs	GGA	3.614	-0.614	3.000
	GGA+U (AL)	3.880	-0.880	3.000
	GGA+U (AMF)	3.541	-0.541	3.000
MnAs	GGA	4.173	-0.311	3.862
	GGA+U (AL)	4.476	-0.476	3.999
	GGA+U (AMF)	3.979	-0.326	3.652

atoms to the N(C) atoms resulting to huge values of the atom-resolved spin moments. This state is obviously an artifact of the method. We cannot explain the origin of this behavior but starting from various configurations all calculations involving the AL functional converged to the same results and thus the breakdown of the AL should be attributed to its characteristics.

The second family of binary compounds under study are the binary VAs, CrAs, and MnAs transition metal pnictides. The first observation of such a compound being half-metal was made in 2000 when Akinaga and his collaborators managed to grow multilayers of CrAs/GaAs.<sup>53</sup> CrAs was found to adopt the zincblende structure of GaAs and was predicted to be a half-metal with a total spin magnetic moment of 3  $\mu_B$  in agreement with experiments.<sup>53</sup> Several studies followed this initial discovery, and electronic structure calculations have confirmed that also similar binary XY compounds, where X is an early transition-metal atom and Y an *sp* element, should be half-metals and the total spin magnetic moment follows a SP rule similar to d<sup>0</sup>-ferromagnets being

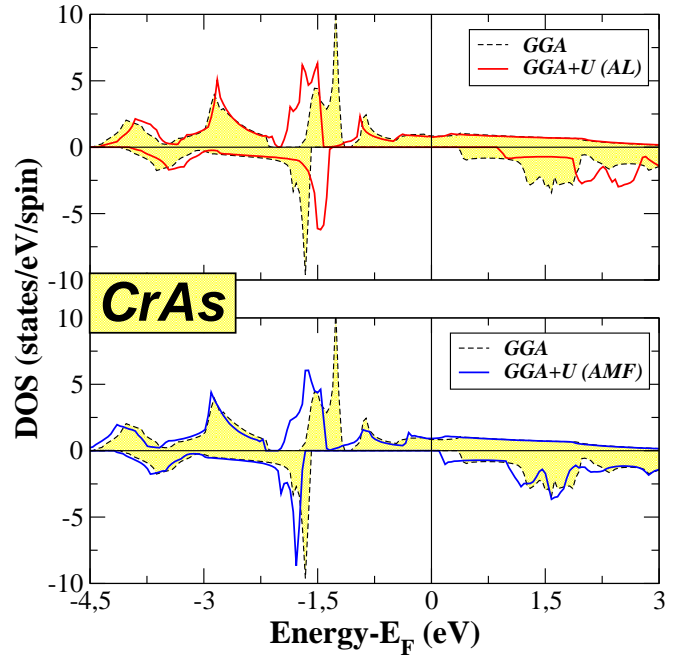


FIG. 1: (color online) Total density of states (DOS) as a function of the energy for the CrAs compound within the GGA+U method using both the atomic-limit (AL) and the around-mean-field (AMF) functionals for the double-counting term. GGA+U results are compared to the GGA calculated DOS. The zero in the energy axis has been set to the Fermi level. Positive(negative) values of the DOS correspond to the majority(minority)-spin electrons.

now equal to  $Z_t - 8$ .<sup>54,55</sup>

In Table I we gathered all the calculated spin magnetic moments. GGA gives a half-metallic state for VAs and CrAs, while for MnAs the Fermi level is slightly above the minority-spin energy gap and the total spin magnetic moment slightly smaller than the ideal value of 4  $\mu_B$  for half-metallicity to occur. These results have been largely discussed in literature.<sup>54,55</sup> For both VAs and CrAs, GGA+U self-consistent calculations yield a half-metallic state within both AL and AMF functionals with the same total spin magnetic moment but with substantial variations of the atom-resolved spin magnetic moments. For MnAs the use of AL functional leads to a half-metallic state contrary to AMF for which the Fermi level is above the minority-spin gap. Overall AL leads to larger absolute values of the atomic spin moments with respect to GGA while AMF leads to smaller values. This behavior of the atomic spin magnetic moments confirms the conclusion in Ref. 29 that AMF gives the magnetic state a large energy penalty with respect to AL.

Since DOS present similar trends between the three transition metal binary compounds, we present in Fig. 1 the calculated DOS per formula unit for CrAs. In the upper panel we compare the GGA+U calculated DOS within the AL functional to the usual GGA calculated DOS, and in the lower panel we present a similar graph for the AMF case. In the presented energy Cr DOS dom-

inates. GGA produces a large minority-spin gap with a large exchange splitting between the occupied majority-spin bands and the unoccupied minority-spin bands and thus strong tendency to magnetism manifested also by the large ( $\sim 3.6 \mu_B$ ) Cr spin moment. The use of the AL double-counting functional in the GGA+U calculations lead to an almost rigid shift of the minority spin DOS towards higher energies, while in the majority-spin DOS only the double-degenerate  $e_g$  states at about -1.5 eV move lower in energy (see Ref. 54 for a discussion of the character of the bands). In the case of AMF the majority-spin band structure shows a similar behavior with respect to the GGA results as the AL case. But in the minority-spin band structure the tendency is the opposite now. Since AMF does not favor magnetism as strongly as AL, the minority-spin band structure now presents an almost rigid shift towards lower energy values. These findings also explain the behavior of the MnAs compound. In the case of AL the minority-spin band structure moves towards higher energy values and the Fermi level now moves within the gap and half-metallicity appears.

## B. Heusler compounds

Heusler compounds are a huge family of intermetallic compounds presenting various types of electronic and magnetic behaviors.<sup>56,57</sup> Several among them are half-metallic ferromagnets/ferrimagnets/antiferromagnets and are of particular interest due to their very high Curie temperatures, which usually exceed 1000 K, making them ideal for applications.<sup>8</sup> There are four main families of Heusler compounds: (i) the semi-Heuslers also known as half-Heuslers like NiMnSb which have the chemical type XYZ with X and Y being transition metal atoms, (ii) the usual full Heuslers like  $\text{Co}_2\text{MnSi}$  with the chemical type  $\text{X}_2\text{YZ}$  where the valence of X is larger than the valence of Y and the two X atoms are equivalent, (iii) the quaternary Heuslers like  $(\text{CoFe})\text{MnSi}$  which present similar properties with the full-Heuslers, and finally (iv) the so-called inverse-Heuslers, like  $\text{Cr}_2\text{CoGa}$  which have also the chemical type  $\text{X}_2\text{YZ}$  but now the valence of X is smaller than the valence of Y and due to the change of the sequence of atoms in the unit cell the two X atoms are no more equivalent.<sup>56,57</sup> We present results for all families of compounds with the exception of quaternary-Heuslers which present similar behavior to the full-Heuslers and for which no Hubbard parameters have been derived in Ref. 32.

### 1. Semi-Heuslers

The first family of Heusler compounds for which we will present results are the semi-Heuslers. The first compound that was predicted to be a half-metal was actually a semi-Heusler, NiMnSb.<sup>4</sup> Their total spin magnetic moment follows also a SP rule being  $Z_t - 18$  (for an ex-

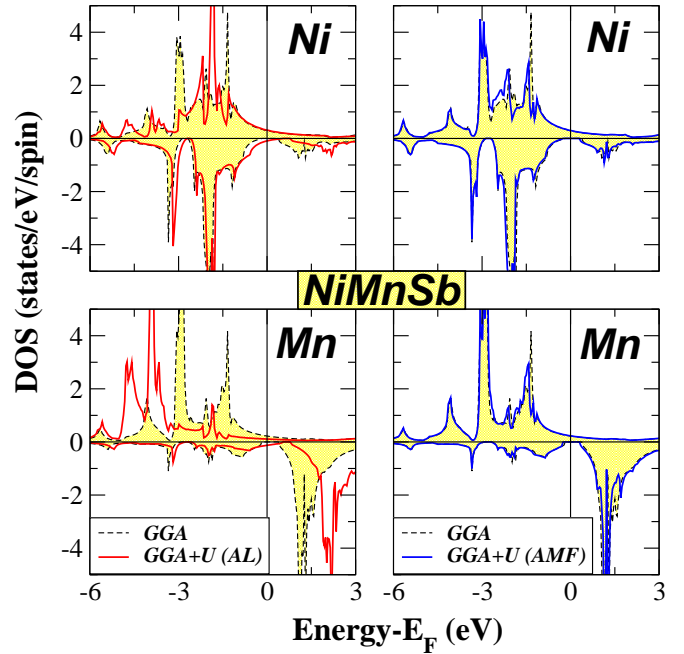


FIG. 2: (color online) Ni and Mn atom-resolved DOS in NiMnSb. Details as in Fig. 1.

tended discussion see Ref. 58). In Table II we have gathered our calculated spin magnetic for all studied cases and for three compounds FeMnSb, CoMnSb and NiMnSb (note that for FeMnSb we were not able to converge the GGA+U calculations using the AMF functional). As we move from one compound to the other, the total number of valence electrons increases by one and so does the GGA calculated total spin magnetic moment. Mn atoms in all case possess a large value of spin magnetic moment which starts from  $\sim 3.4 \mu_B$  in FeMnSb and exceeds  $4 \mu_B$  in NiMnSb. As we increase the total number of valence electrons the spin magnetic of the X atoms also increases being  $\sim 1.3 \mu_B$  for Fe,  $-0.34 \mu_B$  for Co and  $0.14 \mu_B$  for Ni in the corresponding compounds. The GGA calculated DOS, presented in Fig. 2 for NiMnSb, has been studied in detail in literature and it is mainly characterized by the large exchange splitting between the occupied majority-spin and the unoccupied minority-spin  $d$ -states at the Mn site which together with the very small weight of the occupied minority-spin states are responsible for the large Mn spin magnetic moments. This feature is common for all three studied compounds and has been already observed in literature.<sup>58–60</sup>

The self-consistent GGA+U calculations using the AMF functional for the CoMnSb and NiMnSb compounds produced a similar picture to the GGA calculations. The total spin magnetic moment, as shown in Table II remains identical to the GGA case and the atom-resolved spin magnetic moments only scarcely changed. This is also reflected on the Ni and Mn resolved DOS for NiMnSb in Fig. 2 where the GGA+U within AMF calculated DOS is almost identical to the GGA calculated DOS. The effect of the use of the AL functional is more

TABLE II: Similar to Table I for the semi-Heusler compounds crystallizing in the  $C1_b$  lattice structure having the XYZ chemical formula.

Comp.	Functional	$m_X$	$m_Y$	$m_Z$	$m_{\text{total}}$
FeMnSb	GGA	-1.279	3.374	-0.095	2.000
	GGA+U(AL)	-2.274	4.559	0.042	2.327
CoMnSb	GGA	-0.340	3.568	-0.227	3.000
	GGA+U (AL)	-1.264	4.520	-0.186	3.068
	GGA+U (AMF)	-0.358	3.535	-0.177	3.000
NiMnSb	GGA	0.143	4.031	-0.174	3.999
	GGA+U (AL)	-0.087	4.553	-0.301	4.164
	GGA+U (AMF)	0.144	4.026	-0.171	3.999

drastic. As shown in Fig. 2 GGA+U within the AL functional compared to usual GGA leads to large modifications of the DOS of the transition metal atoms. In the case of Mn, the exchange splitting between the occupied majority-spin and the unoccupied minority-spin states increase considerably. In the majority-spin band structure of Mn, the occupied states move lower in energy and as a result they are no more in the same energy with the Ni majority-spin states. This leads to a weaker hybridization between the  $d$  states of Ni and Mn atoms and in the Ni DOS the width of the majority bands becomes smaller as a result of the weaker hybridization effects. Almost all the weight of the occupied minority-spin band structure is located at the Ni atoms while almost all unoccupied minority-spin states are located at the Mn atom. Thus there is almost no hybridization between the minority-spin  $d$ -states of Ni and Mn and the former are not affected by the shift of the later to larger energy values being identical to the GGA case. These changes in DOS are also reflected on the spin magnetic moments in Table II. The larger tendency to magnetism within AL compared to AMF leads to slightly larger total spin magnetic moments which deviate from the ideal integer values of the SP rule and the Fermi level is located slightly below the minority-spin energy gap. In the case of FeMnSb and CoMnSb, both the absolute values of the Fe(Co) and Mn spin magnetic moments increase by about  $1 \mu_B$  almost cancelling each other. In the case of NiMnSb the variations in the atomic spin magnetic moments are considerably smaller since almost all Ni  $d$ -states are occupied in all studied cases. But even for NiMnSb the Mn spin moment increases by  $\sim 0.5 \mu_B$  and the Ni spin moment decrease by about  $0.3 \mu_B$ . The Sb atoms in all cases also present changes in their atomic spin magnetic moments between the various calculations although these variations are considerably smaller than for the transition metal atoms.

## 2. Full-Heuslers

The second family of Heusler compounds which may present half-metallicity are the so-called usual full-Heuslers crystallizing in the cubic  $L2_1$  structures. Half-

TABLE III: Similar to Table I for the full-Heusler compounds crystallizing in the  $L2_1$  lattice structure having the  $X_2YZ$  chemical formula.

Comp.	Functional	$m_X$	$m_Y$	$m_Z$	$m_{\text{total}}$
$Mn_2VAl$	GGA	-1.670	1.227	0.113	-1.999
	GGA+U (AL)	-4.102	3.169	0.483	-4.551
	GGA+U (AMF)	-1.798	1.527	0.079	-1.990
$Mn_2VSi$	GGA	-0.801	0.557	0.060	-0.985
	GGA+U (AL)	-2.248	2.759	0.376	-1.362
$Co_2CrAl$	GGA	0.737	1.684	-0.160	2.999
	GGA+U (AMF)	0.965	1.222	-0.153	3.000
$Co_2CrSi$	GGA	0.934	2.242	-0.111	4.000
	GGA+U (AL)	0.871	2.525	-0.267	4.000
	GGA+U (AMF)	0.890	2.187	0.031	4.000
$Co_2MnAl$	GGA	0.673	2.910	-0.231	4.025
	GGA+U (AL)	1.381	4.176	-0.501	6.438
	GGA+U (AMF)	1.048	1.998	-0.096	3.999
$Co_2MnSi$	GGA	0.972	3.195	-0.140	4.999
	GGA+U (AL)	0.732	3.954	-0.338	5.080
	GGA+U (AMF)	0.987	3.020	-0.004	5.000
$Co_2FeAl$	GGA	1.163	2.870	-0.203	4.999
	GGA+U (AL)	1.188	3.326	-0.520	5.177
	GGA+U (AMF)	1.216	2.673	-0.105	4.999
$Co_2FeSi$	GGA	1.327	2.926	-0.042	5.539
	GGA+U (AL)	1.375	3.450	-0.201	5.999

metallicity can be combined either with the appearance of ferrimagnetism, when the X atoms in the  $X_2YZ$  is the Mn one, or with ferromagnetism when X is Co. In all cases the total spin magnetic moment in  $\mu_B$  follows a SP rule being  $Z_t - 24$ .<sup>61</sup> In Table III we have gathered the calculated spin magnetic moments for all studied compounds with both GGA and GGA+U methods using both the AL and AMF double-counting functional in the later case. When one case is missing in the table, this is due to the fact that we were not able to get convergence irrespectively of the starting input which we have used.

First, we will discuss our results on the half-metallic ferrimagnetic  $Mn_2VAl$  and  $Mn_2VSi$  compounds where the total spin magnetic moments is negative since the total number of valence electrons is less than 24. Moreover the Mn spin magnetic moments are antiferromagnetically coupled to the V spin moments due to their small distance.<sup>61</sup> In the case of  $Mn_2VAl$ , GGA+U calculations within AMF produced similar spin moments and DOS to the GGA case; we were not able to converge GGA+U within AMF for the  $Mn_2VSi$  compound. For both compounds the use of AL double-counting functional produced unphysical results similar to the case of  $d^0$ -ferromagnets in Sec. IIIB. The use of AL tripled, with respect to the GGA case, the absolute values of the spin magnetic moments of the transition metal atoms in  $Mn_2VA$ ; in the case of V in  $Mn_2VSi$  the increase is almost 600%. Thus the use of AL for the half-metallic ferrimagnetic Heusler compounds obviously is inadequate.

In the case of ferromagnetic full-Heuslers containing Co the effect of using both AMF and AL on the calculated electronic and magnetic properties is more complex

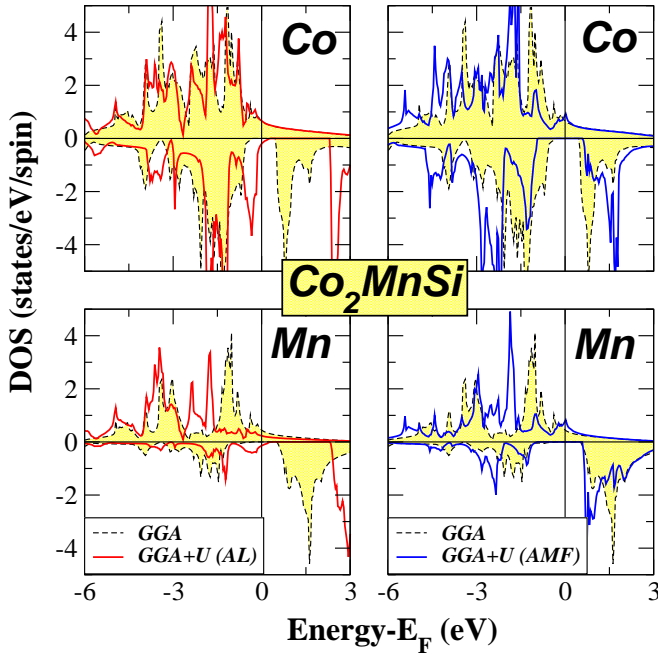


FIG. 3: (color online) Co and Mn atom-resolved DOS in  $\text{Co}_2\text{MnSi}$ . Details as in Fig. 1.

than in all the previously studied cases. When Y is Cr ( $\text{Co}_2\text{CrAl}$  and  $\text{Co}_2\text{CrSi}$ ) both AL and AMF yielded a perfect half-metallic state with the total spin magnetic moment being equal to the ideal values predicted by the SP rule as shown in Table III. When Y is Mn ( $\text{Co}_2\text{MnAl}$  and  $\text{Co}_2\text{MnSi}$ ) AMF produced a half-metallic states and both atom-resolved and total spin magnetic moments were close to the GGA case, but AL led to a considerable increase of the Mn spin moment similarly to the semi-Heuslers. The increase of the Mn spin moment within AL led to an increase also of the total spin magnetic moment which is only  $0.80 \mu_B$  for  $\text{Co}_2\text{MnSi}$  but reaches the  $\sim 1.4 \mu_B$  for  $\text{Co}_2\text{MnAl}$ . When Y is Fe ( $\text{Co}_2\text{FeAl}$  and  $\text{Co}_2\text{FeSi}$ ) the behavior of the spin moments with respect to the GGA results is similar within both AL and AMF to the case where Y is Mn. Moreover in the case of  $\text{Co}_2\text{FeSi}$  which is not half-metallic within GGA, the use of GGA+U combined with AL leads to a total spin magnetic moment of  $6 \mu_B$  and to a half-metallic state as shown also in Ref. 13. Although the GW scheme<sup>62</sup> produced similar results to the GGA+ calculations, correlations in this materials are still an open issue since recent results by Meinert and collaborators show that a self-consistent calculation fixing the total spin magnetic moment to  $6 \mu_B$  reproduces more accurately the position of the band with respect to available experimental data.<sup>63</sup>

To understand the behavior of the spin moments we have to examine in detail the behavior of the DOS. Since the trends when either AMF or AL is employed are similar for all six ferromagnetic Co-based full-Heuslers under study, we will use  $\text{Co}_2\text{MnSi}$  as an example and in Fig. 3 we present the Co and Mn resolved DOS. When the

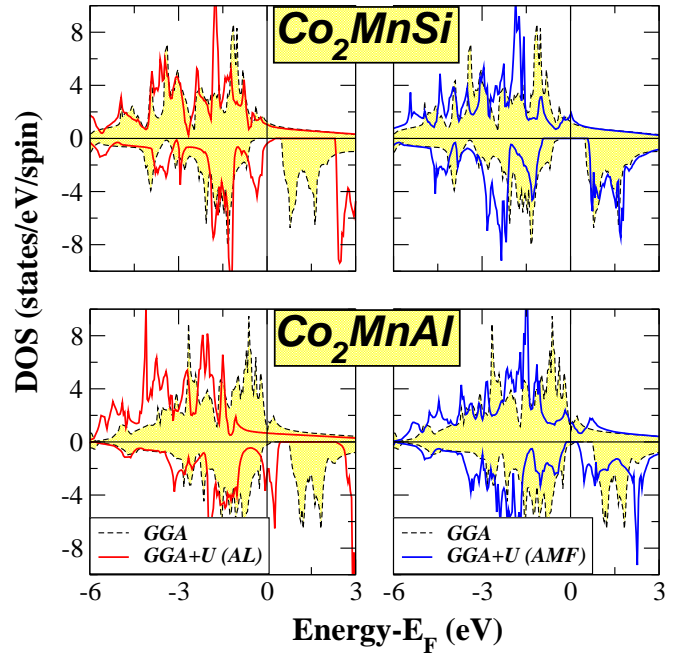


FIG. 4: (color online) Total DOS per formula unit for the  $\text{Co}_2\text{MnSi}$  and  $\text{Co}_2\text{MnAl}$  compounds. Details as in Fig. 1.

GGA+U combined with AMF is used (left panel) there is a significant change in the DOS unlikely all other families of half-metallic compounds discussed above. AMF enhances the tendency to magnetism with respect to GGA. For the Mn atom the occupied majority spin states shift lower in energy but the minority-spin energy gap in the Mn DOS remains unchanged. Through hybridization also the Co majority-spin DOS shifts lower in energy and so do also the occupied Co minority-spin states. This leads to an increase of the energy gap in the Co minority-spin band structure. Since as explained in Ref. 61 Co atoms present in usual GGA calculations a much smaller gap than the Mn atoms and thus determine the energy gap in the total DOS, the opening of the former further stabilizes the half-metallic state.

The GGA+U method combined with AL even further enhances the tendency to magnetism with respect to AMF as concluded in Ref. 29. In the case of Mn atoms the exchange splitting between the occupied majority-spin and unoccupied minority-spin states is greatly enhanced as for Mn in  $\text{NiMnSb}$  and thus the energy gap becomes much larger. As a side-effect some weight in the minority-spin band structure appears just below the Fermi level. Thus although with respect to the GGA case, AL opens the gap the Fermi level is located close to the left edge of the gap instead of the middle in the GGA case. Co DOS follows through hybridization the behavior of the Mn  $d$ -states and the gap is now also much larger but the occupied minority-spin states move closer to the Fermi level which now just crosses the states just below the low-energy edge of the gap and the total spin magnetic moment within AL is slightly larger than the ideal value of  $5 \mu_B$ .



TABLE IV: Similar to Table I for the full-Heusler compounds crystallizing in the inverse  $XA$  lattice structure having the  $\text{Cr}_2\text{YZ}$  chemical formula, where the two Cr atoms occupy sites of different symmetry (see text).

Comp.	Functional	$m_{\text{Cr}A}$	$m_{\text{Cr}B}$	$m_Y$	$m_Z$	$m_{\text{total}}$
$\text{Cr}_2\text{FeGe}$	GGA	-1.454	1.753	-0.313	0.027	0.012
	GGA+U(AL)	-4.162	4.672	-1.054	0.551	0.006
$\text{Cr}_2\text{CoGa}$	GGA	-2.680	1.973	0.379	-0.014	0.069
	GGA+U (AL)	-4.860	4.137	1.160	-0.082	0.520

In the case of  $\text{Co}_2\text{MnAl}$  the change in the spin magnetic moments is larger within both AL and AMF functionals. As shown in Fig. 4, although we just change Al for Si in  $\text{Co}_2\text{MnSi}$ , the AMF DOS shows a different tendency with respect to the energy gap. The exchange splitting between occupied majority and unoccupied minority spin states is smaller, and within AMF the gap is smaller than within GGA showing the contrary tendency to  $\text{Co}_2\text{MnSi}$  where AMF produced a larger gap with respect to GGA. For  $\text{Co}_2\text{MnAl}$  within usual GGA the Fermi level is close to the left edge of the gap while for  $\text{Co}_2\text{MnSi}$  it is located at the middle of the gap. Thus in the case of AL based calculations the shift of the Co occupied minority spin states towards higher energies for  $\text{Co}_2\text{MnAl}$ , discussed just above also for  $\text{Co}_2\text{MnSi}$ , leads to the loss of the half-metallicity since now the Fermi level crosses the occupied minority-spin states. The other AL-based Heuslers ( $\text{Co}_2\text{CrAl}$  and  $\text{Co}_2\text{FeAl}$ ) exhibit within GGA a DOS around the minority-spin energy gap similar to  $\text{Co}_2\text{MnSi}$  and not  $\text{Co}_2\text{MnAl}$  and thus the increase in their total spin magnetic moment within AL is much smaller than for  $\text{Co}_2\text{MnAl}$ .

### 3. Inverse-Heuslers

The last family of potential half-metallic Heusler compounds are the so-called inverse Heusler compounds.<sup>64</sup> Among these half-metals the most interesting are the so-called fully-compensated ferrimagnets (also known as half-metallic antiferromagnets) like  $\text{Cr}_2\text{FeGe}$  and  $\text{Cr}_2\text{CoGa}$ . These materials are of special interest since they combine half-metallicity to a zero total net magnetization and thus are ideal for spintronic/magnetoelectronic devices due to the vanishing external stray fields created by them.<sup>65</sup> We should note that films of  $\text{Cr}_2\text{CoGa}$  have been grown experimentally<sup>66</sup> and this compounds has been predicted to exhibit extremely large Curie temperature.<sup>67</sup> As shown in Table IV GGA yields for both  $\text{Cr}_2\text{FeGe}$  and  $\text{Cr}_2\text{CoGa}$  compounds a total spin magnetic moment close to zero (for an extended discussion on the half-metallic inverse Heuslers

see Ref. 64). Note that we have two inequivalent Cr atoms in these compounds denoted by the superscripts  $A$  and  $B$  in Table IV. We were not able to converge the GGA+U self-consistent calculations using the AMF double-counting functional. For the AL functional although the total spin magnetic moment stays close to zero, the absolute values of the Cr spin magnetic moments are about doubled leading to an unphysical situations. Thus for these materials the use of GGA+U combined with AL is not able to produce a reasonable description of the electronic structure as was also the case for the semi-Heuslers and the ferrimagnetic full-Heuslers.

## IV. CONCLUSIONS

We have studied the electronic and magnetic properties of 20 half-metallic magnets performing self-consistent GGA+U calculations using both the atomic-limit (AL) and around-mean-field (AMF) functionals for the double counting term and compared them to the usual GGA calculations. Overall the use of AMF produced results similar to the usual GGA calculations. The effect of AL was diversified depending on the studied material. In the case of  $d^0$ -ferromagnets, semi-Heuslers, ferrimagnetic full-Heuslers and inverse Heuslers the use of AL leads to unrealistic electronic and magnetic properties of the studied compounds and thus its use is not justified. On the other hand in the case of transition-metal binary compounds and usual ferromagnetic full-Heusler compounds the use of AL enhanced the tendency towards magnetism with respect to both GGA and GGA+U combined with AMF. Depending on the position of the Fermi level, there were cases like MnAs and  $\text{Co}_2\text{FeSi}$  for which AL produced a half-metallic state contrary to GGA and GGA+U combined with AMF, cases like VAs, CrAs and  $\text{Co}_2\text{CrSi}$  where all three methods produced a half-metallic state, and cases like  $\text{Co}_2\text{MnAl}$ ,  $\text{Co}_2\text{MnSi}$  and  $\text{Co}_2\text{FeAl}$  where the use of AL led to the loss of half-metallicity.

Methods based on the combination of the usual density functional theory (DFT)-based codes and of the Hubbard  $U$ -Hund's exchange  $J$  are widely used to investigate the properties of strongly correlated materials. Our results suggest that especially in the case of half-metallic magnets the choice for the double counting functional used to subtract the part from the DFT total energy, which is associated to the Coulomb repulsion between the correlated orbitals, plays a decisive role on the obtained results. Thus the study of correlations in half-metallic magnets is still an open issue and further studies are needed to establish the predictive power of methods based on the  $U$  and  $J$  parameters like GGA+U or LDA+DMFT methods.

\* Electronic address: galanakis@upatras.gr

<sup>1</sup> I. Žutić, J. Fabian, and S. Das Sarma, Rev. Mod. Phys.

- 76**, 323 (2004).
- <sup>2</sup> M. I. Katsnelson, V. Yu. Irkhin, L. Chioncel, A. I. Lichtenstein, and R.A. de Groot, *Rev. Mod. Phys.* **80**, 315 (2008).
  - <sup>3</sup> K. Sato, L. Bergqvist, J. Kudrnovský, P. H. Dederichs, O. Eriksson, I. Turek, B. Sanyal, G. Bouzerar, H. Katayama-Yoshida, V. A. Dinh, T. Fukushima, H. Kizaki, and R. Zeller, *Rev. Mod. Phys.* **82**, 1633 (2010).
  - <sup>4</sup> R. A. de Groot, F. M. Mueller, P. G. van Engen, and K. H. J. Buschow, *Phys. Rev. Lett.* **50**, 2024 (1983).
  - <sup>5</sup> W. E. Pickett and H. Eschrig, *J. Phys.: Condens. Matter* **19**, 315203 (2007).
  - <sup>6</sup> C. Felser, G. H. Fecher, and B. Balke, *Angew. Chem. Int. Ed.* **46**, 668 (2007).
  - <sup>7</sup> T. Graf, C. Felser, and S. S. P. Parkin, *Progress in Solid State Chemistry* **39**, 1 (2011).
  - <sup>8</sup> A. Hirohata and K. Takamashi, *J. Phys. D: Appl. Phys.* **47**, 193001 (2014).
  - <sup>9</sup> J.P. Perdew and Y. Wang, *Phys. Rev. B* **45** (1992) 13244.
  - <sup>10</sup> J. P. Perdew, K. Burke, and M. Ernzerhof, *Phys. Rev. Lett.* **77**, 3865 (1996).
  - <sup>11</sup> K. Karlsson, F. Aryasetiawan, and O. Jepsen, *Phys. Rev. B* **81**, 245113 (2010).
  - <sup>12</sup> I. V. Solovyev, *J. Phys.: Condens. Matter* **20**, 293201 (2008).
  - <sup>13</sup> H. M. Kandpal, G. H. Fecher, C. Felser, and G. Schönhense, *Phys. Rev. B* **73**, 094422 (2006).
  - <sup>14</sup> A. Yamasaki, L. Chioncel, A. I. Lichtenstein, and O. K. Andersen, *Phys. Rev. B* **74**, 024419 (2006).
  - <sup>15</sup> J. Minár, *J. Phys.: Condens. Matter* **23**, 253201 (2011).
  - <sup>16</sup> F. Lechermann, A. Georges, A. Poteryaev, S. Biermann, M. Posternak, A. Yamasaki, and O. K. Andersen, *Phys. Rev. B* **74**, 125120 (2006).
  - <sup>17</sup> L. Chioncel, Y. Sakuraba, E. Arrigoni, M. I. Katsnelson, M. Oogane, Y. Ando, T. Miyazaki, E. Burzo, and A. I. Lichtenstein *Phys. Rev. Lett.* **100**, 086402 (2008).
  - <sup>18</sup> L. Chioncel, M. I. Katsnelson, R. A. de Groot, and A. I. Lichtenstein, *Phys. Rev. B* **68**, 144425 (2003).
  - <sup>19</sup> S. Chadov, J. Minár, H. Ebert, A. Perlov, L. Chioncel, M. I. Katsnelson, and A. I. Lichtenstein, *Phys. Rev. B* **74**, 140411(R) (2006).
  - <sup>20</sup> H. Allmaier, L. Chioncel, E. Arrigoni, M. I. Katsnelson, and A. I. Lichtenstein, *Phys. Rev. B* **81**, 054422 (2010).
  - <sup>21</sup> L. Chioncel, E. Arrigoni, M. I. Katsnelson, and A. I. Lichtenstein, *Phys. Rev. Lett.* **96**, 137203 (2006).
  - <sup>22</sup> L. Chioncel, E. Arrigoni, M. I. Katsnelson, and A. I. Lichtenstein *Phys. Rev. B* **79**, 125123 (2009).
  - <sup>23</sup> L. Chioncel, Ph. Mavropoulos, M. Ležaić, S. Blügel, E. Arrigoni, M. I. Katsnelson, and A. I. Lichtenstein, *Phys. Rev. Lett.* **96**, 197203 (2006).
  - <sup>24</sup> L. Chioncel, M. I. Katsnelson, G. A. de Wijs, R. A. de Groot, and A. I. Lichtenstein, *Phys. Rev. B* **71**, 085111 (2005).
  - <sup>25</sup> L. Chioncel, I. Leonov, H. Allmaier, F. Beuiseanu, E. Arrigoni, T. Jurcut, and W. Ptz, *Phys. Rev. B* **83**, 035307 (2011).
  - <sup>26</sup> V. I. Anisimov, J. Zaanen, and O. K. Andersen, *Phys. Rev. B* **44**, 943 (1991).
  - <sup>27</sup> V. I. Anisimov, I. V. Solovyev, M. A. Korotin, M. T. Czyżyk, and G. A. Sawatzky, *Phys. Rev. B* **48**, 16929 (1993).
  - <sup>28</sup> M. T. Czyżyk and G. A. Sawatzky, *Phys. Rev. B* **49**, 14211 (1994).
  - <sup>29</sup> E. R. Ylvisaker, W. E. Pickett, and K. Koepnik, *Phys. Rev. B* **79**, 035103 (2009).
  - <sup>30</sup> K. Koepnik and H. Eschrig, *Phys. Rev. B* **59**, 1743 (1999).
  - <sup>31</sup> K. Koepnik, Full Potential Local Orbital Minimum Basis Bandstructure Scheme Users Manual (<http://www.fplo.de/download/doc.pdf>).
  - <sup>32</sup> E. Şaşıoğlu, I. Galanakis, C. Friedrich, and S. Blügel, *Phys. Rev. B* **88**, 134402 (2013).
  - <sup>33</sup> F. Aryasetiawan, M. Imada, A. Georges, G. Kotliar, S. Biermann, and A. I. Lichtenstein, *Phys. Rev. B* **70**, 195104 (2004).
  - <sup>34</sup> F. Aryasetiawan, K. Karlsson, O. Jepsen, and U. Schönberger, *Phys. Rev. B* **74**, 125106 (2006).
  - <sup>35</sup> T. Miyake and F. Aryasetiawan, *Phys. Rev. B* **77**, 085122 (2008); T. Miyake, F. Aryasetiawan, and M. Imada *Phys. Rev. B* **80**, 155134 (2009).
  - <sup>36</sup> E. Şaşıoğlu, C. Friedrich, and S. Blügel, *Phys. Rev. B* **83**, 121101(R) (2011).
  - <sup>37</sup> P. H. Dederichs, S. Blügel, R. Zeller, and H. Akai, *Phys. Rev. Lett.* **53**, 2512 (1984).
  - <sup>38</sup> V. I. Anisimov and O. Gunnarsson, *Phys. Rev. B* **43**, 7570 (1991).
  - <sup>39</sup> M. Cococcioni and S. de Gironcoli, *Phys. Rev. B* **71**, 035105 (2005).
  - <sup>40</sup> K. Nakamura, R. Arita, Y. Yoshimoto, and S. Tsuneyuki, *Phys. Rev. B* **74**, 235113 (2006).
  - <sup>41</sup> K. Kusakabe, M. Geshi, H. Tsukamoto, and N. Suzuki, *J. Phys.:Condens. Matter* **16**, S5639 (2004).
  - <sup>42</sup> A. Laref, E. Şaşıoğlu, and I. Galanakis, *J. Phys.:Condens. Matter* **23**, 296001 (2011).
  - <sup>43</sup> G. Y. Gao, K. L. Yao, and N. Li, *J. Phys.:Condens. Matter* **23**, 075501 (2011).
  - <sup>44</sup> M. Sieberer, J. Redinger, S. Khmelevskyi, and P. Mohn, *Phys. Rev. B* **73**, 024404 (2006).
  - <sup>45</sup> M. Geshi, K. Kusakabe, H. Nagara, and N. Suzuki, *Phys. Rev. B* **76**, 054433 (2007).
  - <sup>46</sup> K. Özdoğan, E. Şaşıoğlu, and I. Galanakis, *J. Appl. Phys.* **111**, 113918 (2012).
  - <sup>47</sup> G. Y. Gao and K. L. Yao, *Appl. Phys. Lett.* **91**, 082512 (2007).
  - <sup>48</sup> G. Y. Gao, K. L. Yao, E. Şaşıoğlu, L. M. Sandratskii, Z. L. Liu, and J. L. Jiang, *Phys. Rev. B* **75**, 174442 (2007).
  - <sup>49</sup> S. Dong and H. Zhao, *Appl. Phys. Lett.* **98**, 182501 (2011).
  - <sup>50</sup> J. C. Slater, *Phys. Rev.* **49**, 931 (1936).
  - <sup>51</sup> L. Pauling, *Phys. Rev.* **54**, 899 (1938).
  - <sup>52</sup> <http://www.flapw.de>
  - <sup>53</sup> H. Akinaga, T. Manago, and M. Shirai, *Jpn. J. Appl. Phys.* **39**, L1118 (2000).
  - <sup>54</sup> I. Galanakis and P. Mavropoulos, *Phys. Rev. B* **67**, 104417 (2003).
  - <sup>55</sup> Ph. Mavropoulos and I. Galanakis, *J. Phys. Condens. Matter* **19**, 315221 (2007).
  - <sup>56</sup> P. J. Webster and K. R. A. Ziebeck, in *Alloys and Compounds of d-Elements with Main Group Elements. Part 2.*, edited by H. R. J. Wijn, Landolt-Börnstein, New Series, Group III, Vol. 19, Pt.c (Springer-Verlag, Berlin 1988), pp. 75-184.
  - <sup>57</sup> K. R. A. Ziebeck and K.-U. Neumann, in *Magnetic Properties of Metals*, Edited H. R. J. Wijn, Landolt-Börnstein, New Series, Group III, Springer, Berlin (2001), Vol. 32/c, pp. 64-414.
  - <sup>58</sup> I. Galanakis, P. H. Dederichs, and N. Papanikolaou, *Phys. Rev. B* **66**, 134428 (2002).
  - <sup>59</sup> R. A. De Groot, A. M. van der Kraan, K. H. J. Buschow,



- J. Magn. Magn. Mater. **61**, 330 (1986).
- <sup>60</sup> H. M. Huang, S. J. Luo, K. L. Yao, Physica B **406**, 1368 (2011).
- <sup>61</sup> I. Galanakis, P. H. Dederichs, and N. Papanikolaou, Phys. Rev. B **66**, 174429 (2002).
- <sup>62</sup> M. Meinert, C. Friedrich, G. Reiss, and S. Blügel, Phys. Rev. B **86**, 245115 (2012).
- <sup>63</sup> M. Meinert, J.-M. Schmalhorst, M. Glas, G. Reiss, E. Arenholz, T. Böhnert, and K. Nielsch, Phys. Rev. B **86**, 054420 (2012); M. Meinert, Phys. Rev. B **87**, 045103 (2013).
- <sup>64</sup> S. Skaftouros, K. Özdoğan, E. Şaşıoğlu, and I. Galanakis, Phys. Rev. B **87**, 024420 (2013).
- <sup>65</sup> H. van Leuken and R. A. de Groot, Phys. Rev. Lett. **74**, 1171 (1995).
- <sup>66</sup> T. Graf, F. Casper, J. Winterlik, B. Balke, G.H. Fecher, and C. Felser, Z. Anorg. Allg. Chem. **635**, 976 (2009).
- <sup>67</sup> I. Galanakis and E. Şaşıoğlu, Appl. Phys. Lett. **99**, 052509 (2011).